Green Chemistry

PAPER

View Article Online
View Journal | View Issue

Cite this: *Green Chem.*, 2019, **21**, 4475

A facile strategy to achieve fully bio-based epoxy thermosets from eugenol†

Chien-Han Chen,[a,b] Shih-Huang Tung,[a,b] Ru-Jong Jeng,*[a,b] Mahdi M. Abu-Omar[c] and Ching-Hsuan Lin*[a,d]

Received 11th April 2019,
Accepted 18th July 2019

DOI: 10.1039/c9gc01184f

rsc.li/greenchem

To achieve sustainability, many kinds of bio-based epoxy resins have been developed. However, to the best of our knowledge, a 100% bio-based epoxy thermoset has rarely been reported since it needs both the epoxy resin and curing agent to be bio-based. This work provides a facile strategy to achieve epoxy thermosets with 100% bio-based content. The strategy includes the preparation of four bio-based epoxy resins **1–4** and their thermosets through the self-curing reaction of **1–4**. The epoxy compounds **1–4** were prepared from the esterification of eugenol with succinyl, adipoyl, suberoyl, and 2,5-furan chloride, respectively, followed by the oxidation of the allylic bond. Through NMR, DSC, and FTIR analyses, we confirm that the self-curing reaction of **1–4** occurred through a 4-dimethylpyridine (DMAP)-catalyzed reaction of active esters and epoxides. This work successfully provides a facile strategy to achieve fully bio-based epoxy thermosets.

Introduction

In the past few decades, polymeric materials have mostly relied on petroleum-based chemicals. However, due to environmental concerns and limited resources of petroleum, the development of bio-based polymers has increased in recent years.[1,2] More and more bio-based compounds have been produced from agriculture and other natural resources.[3–11] Epoxy resins, due to their unique properties after curing with curing agents, have been widely used in the fields of coatings, encapsulation, composites and electronic applications.[12,13] To achieve sustainability, many kinds of bio-based epoxy resins[14–17] and curing agents[18–20] have been reported. Epoxy resins derived from catechin,[21] curcumin and resveratrol,[22] resorcinol–acetone products,[23] cardanol,[24] vanillin,[25] and vanillin acid[26] have been reviewed by David *et al.*[27] and Koike.[28] Bio-based thermosetting resins derived from renewable plant oils, cardanol, rosin acid, lignin, glycerol, gallic acid, furan, isosorbide, and itaconic acid have been reviewed by Liu and Zhu *et al.*[29] Webster *et al.*[30–32] also reported the preparation of fully bio-based epoxy thermosets from bio-based epoxidized sucrose soyate and carboxylic acid compounds derived from isosorbide and maleic anhydride.

Eugenol, an oily liquid extracted from certain essential oils, is commonly used as a flavoring agent in food products.[33] Eugenol-rich cinnamon oil makes the most effective natural mosquito repellent.[34] Eugenol has been attracting much attention not only because it can be produced from nature, but also because of its distinctive structure. The phenolic group provides a reaction site for modification such as etherification or esterification, and the allylic group provides a route to prepare epoxy resins through oxidation. Zhang *et al.*,[35] Wang *et al.*,[36–38] Gu *et al.*,[39] and Caillol *et al.*[40] have reported the synthesis of eugenol-based epoxy compounds. However, petrochemical-based curing agents are used to cure the epoxy resins mentioned above, remarkably reducing the bio-based content of the epoxy thermosets. None of them dealt with the self-curing characteristic of the eugenol-based epoxy compounds.

In this work, we provide a facile strategy to achieve 100% bio-based epoxy thermosets. The strategy includes the preparation of four bio-based epoxy compounds **1–4** and their thermosets through the self-curing reaction of **1–4**. The epoxy compounds **1–4** were prepared from the esterification of eugenol with succinyl, adipoyl, suberoyl, and 2,5-furan chloride, respectively, followed by the oxidation of the allylic bond. Since the diacid chlorides were obtained from the corresponding renewable acids,[41–44] epoxy compounds **1–4** are thought to be fully bio-based, and their self-cured thermosets are definitely fully bio-based. Through NMR, DSC, and FTIR analyses, we confirm that the self-curing reaction of **1–4** occurred through a 4-dimethylpyridine (DMAP)-catalyzed reaction of active esters and epoxides. Their detailed synthesis, analyses, and properties are reported in this work.

[a]*Advanced Research Center for Green Materials Science and Technology, National Taiwan University, Taipei, Taiwan. E-mail: rujong@ntu.edu.tw, linch@nchu.edu.tw*
[b]*Institute of Polymer Science and Engineering, National Taiwan University, Taipei, Taiwan*
[c]*Department of Chemistry and Biochemistry, University of California, Santa Barbara, California, USA*
[d]*Department of Chemical Engineering, National Chung Hsing University, Taichung, Taiwan*

†Electronic supplementary information (ESI) available. See DOI: 10.1039/c9gc01184f

Experimental

Materials

Eugenol was purchased from Sigma-Aldrich. Succinyl and adipoyl chloride, trimethylamine (TEA), 3-chloroperoxybenzoic acid (*m*CPBA) and 4-dimethylpyridine (DMAP) were purchased from Acros. Suberoyl chloride and glycidyl phenyl ether were purchased from TCI. 4,4′-Methylenedianiline (DDM) was purchased from Chriskev. Sodium sulfite and sodium bicarbonate were purchased from Fluka. 2,5-Furandicarbonyl chloride was prepared according to the literature.[45] Phenyl furan-2-carboxylate was prepared according to the literature.[46] The solvents were of HPLC grade, purchased from a common source and used without further purification.

Characterization

NMR measurements were performed on a Varian Inova 600 NMR. The thermal stability of epoxy thermosets was determined on a PerkinElmer Pyris1 TGA. The analysis was performed under a nitrogen atmosphere. The heating rate was 20 °C min^{-1}. Differential scanning calorimetry measurements were conducted on a PerkinElmer DSC 8000. The heating rate was 10 °C min^{-1}. Dynamic mechanical analysis was performed with a PerkinElmer Pyris Diamond DMA. The heating rate was 5 °C min^{-1}. The dielectric properties were characterized on an Agilent E4991A at 1 GHz at 25 °C. The IR spectra were recorded in the standard wavenumber range of 650–4000 cm^{-1} by using a PerkinElmer RX1 infrared spectrophotometer. The gel content was measured according to the following procedure: "The sample with a known weight (W_i) was immersed at $CHCl_3$ at 25 °C for 24 hours. The sample was then dried at 80 °C in vacuum for 48 hours to achieve a constant weight (W_f)". The gel content is given by the following equation: (W_f/W_i) × 100%. The stress–strain curves were obtained by using EZ-SX at 25 °C; the maximum force of the instrument is 100 Nt.

Synthesis of bis(4-allyl-2-methoxyphenyl) succinate (1a)

Eugenol 26.49 g (64.52 × 2.5 mmol), triethylamine 16.32 g (64.52 × 2.5 mmol) and ethyl acetate 100 mL were introduced into a 250 mL flask equipped with a nitrogen inlet and a stirrer. Succinyl chloride 10.00 g (64.52 mmol) in 50 mL ethyl acetate was added dropwise in an ice bath over 1 h with vigorous agitation and then stirred at 25 °C for another 4 h. The white salt was filtered. The filtrate was extracted with 1 N $NaOH_{(aq)}$ and 1 N $HCl_{(aq)}$, respectively. The organic layer was evaporated and the obtained mixture was washed with hexane; the obtained precipitate was filtered and recrystallized from ethanol, and dried at 60 °C to obtain a white crystal (**1a**) (yield = 83%). ^{1}H-NMR (ppm, $CDCl_3$), δ = 6.94 (2H, H^9), 6.77 (2H, H^5), 6.74 (2H, H^{10}), 5.94 (2H, H^2), 5.08 (4H, H^1), 3.78 (6H, H^6), 3.36 (4H, H^3), 3.02 (4H, H^{12}). ^{13}C-NMR (ppm, $CDCl_3$), δ = 170.38 (C^{11}), 150.74 (C^8), 139.00 (C^7), 137.82 (C^4), 136.99 (C^2), 122.47 (C^9), 120.60 (C^{10}), 116.11 (C^1), 112.63 (C^5), 55.77 (C^6), 40.05 (C^3), 29.07 (C^{12}). Melting point: 88.3–91.7 °C (onset–offset temperature in the DSC thermogram). HR-MS (ESI-MS) *m*/*z*: [Na+] calcd for $C_{24}H_{26}O_6Na$ 433.16; anal. 433.1621. FTIR (KBr): ν (cm^{-1}) = 1756 (C═O stretch of the carbonyl group) and 1638 (C═C stretch of the allylic group).

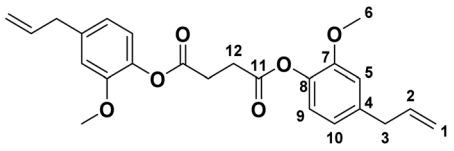

Synthesis of bis(4-allyl-2-methoxyphenyl) adipate (2a)

2a was prepared by using the same procedure as that for **1a** except for succinyl chloride being replaced by adipoyl chloride, and a white crystal **2a** was obtained (yield = 80%). ^{1}H-NMR (ppm, $CDCl_3$), δ = 6.92 (2H, H^9), 6.76 (2H, H^5), 6.74 (2H, H^{10}), 5.94 (2H, H^2), 5.08 (4H, H^1), 3.78 (6H, H^6), 3.36 (4H, H^3), 2.63 (4H, H^{12}), 1.90 (4H, H^{13}). ^{13}C-NMR (ppm, $CDCl_3$), δ = 171.53 (C^{11}), 150.77 (C^8), 138.88 (C^7), 137.89 (C^4), 137.02 (C^2), 122.42 (C^9), 120.59 (C^{10}), 116.10 (C^1), 112.58 (C^5), 55.70 (C^6), 40.05 (C^3), 33.62 (C^{12}), 24.33 (C^{13}). Melting point: 97.9–100.8 °C (onset–offset temperature in the DSC thermogram). HR-MS (ESI-MS) *m*/*z*: [Na+] calcd for $C_{26}H_{30}O_6Na$ 461.19; anal. 461.1929. FTIR (KBr): ν (cm^{-1}) = 1756 (C═O stretch of the carbonyl group) and 1638 (C═C stretch of the allylic group).

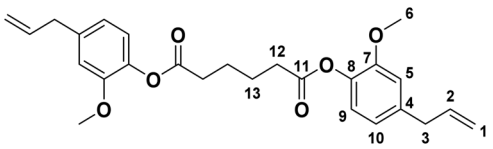

Synthesis of bis(4-allyl-2-methoxyphenyl) octanedioate (3a)

3a was prepared by using the same procedure as that for **1a** except for succinyl chloride being replaced by suberoyl chloride, and a white crystal **3a**) was obtained (yield = 88%). ^{1}H-NMR (ppm, $CDCl_3$), δ = 6.92 (2H, H^9), 6.76 (2H, H^5), 6.74 (2H, H^{10}), 5.94 (2H, H^2), 5.08 (4H, H^1), 3.78 (6H, H^6), 3.36 (4H, H^3), 2.57 (4H, H^{12}), 1.78 (4H, H^{13}), 1.48 (4H, H^{14}). ^{13}C-NMR (ppm, $CDCl_3$), δ = 171.87 (C^{11}), 150.79 (C^8), 138.81 (C^7), 137.91 (C^4), 137.02 (C^2), 122.54 (C^9), 120.59 (C^{10}), 116.07 (C^1), 112.59 (C^5), 55.72 (C^6), 40.04 (C^3), 33.90 (C^{12}), 26.83 (C^{14}), 264.83 (C^{13}). Melting point: 99.9–104.2 °C (onset–offset temperature in the DSC thermogram). HR-MS (ESI-MS) *m*/*z*: [Na+] calcd for $C_{28}H_{34}O_6Na$ 489.22; anal. 489.2238. FTIR (KBr): ν (cm^{-1}) = 1759 (C═O stretch of the carbonyl group) and 1638 (C═C stretch of the allylic group).

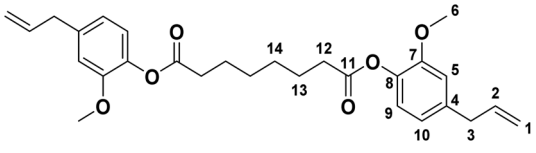

Synthesis of bis(4-allyl-2-methoxyphenyl) furan-2,5-dicarboxylate (4a)

4a was prepared by using the same procedure as that for **1a** except for succinyl chloride being replaced by 2,5-furandicarbonyl chloride, and a white crystal **4a**) was obtained (yield = 81%).

^{1}H-NMR (ppm, $CDCl_3$), δ = 7.44 (2H, H^{13}), 7.05 (2H, H^9), 6.81 (2H, H^5), 6.79 (2H, H^{10}), 5.96 (2H, H^2), 5.09 (4H, H^1), 3.80 (6H, H^6), 3.38 (4H, H^3). ^{13}C-NMR (ppm, $CDCl_3$), δ = 155.84 (C^{11}), 150.76 (C^{12}), 146.54 (C^8), 139.55 (C^7), 137.07 (C^4), 136.88 (C^2), 122.33 (C^9), 120.68 (C^{10}), 119.77 (C^{13}), 116.23 (C^1), 112.77 (C^5), 55.79 (C^6), 40.06 (C^3). Melting point: 101.2–105.3 °C (onset–offset temperature in the DSC thermogram). HR-MS (ESI-MS) *m*/*z*: [Na+] calcd for $C_{26}H_{24}O_7Na$ 471.14; anal. 471.1416. FTIR (KBr): ν (cm^{-1}) = 1761 and 1741 (C=O stretch of the carbonyl group) and 1638 (C=C stretch of the allylic group).

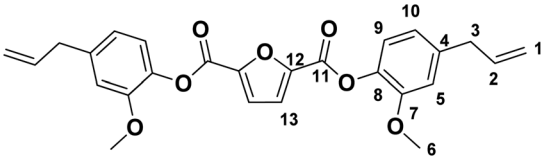

Synthesis of bis(2-methoxy-4-(oxiran-2-ylmethyl)phenyl) succinate (1)

1a 10.00 g (24.36 mmol) and ethyl acetate 200 mL were introduced into a flask equipped with a nitrogen inlet, a stirrer, and a thermocouple. *m*CPBA 21.02 g (24.36 × 5 mmol) was added slowly at 0 °C. The solution was slowly warmed to 40 °C and stirred for 24 hours. The obtained mixture was extracted three times with 10 wt% of $Na_2SO_{3(aq)}$, and three times with 5 wt% of Na_2CO_3. The organic layer was dried over magnesium sulfate, and ethyl acetate was evaporated using a rotary evaporator. A white solid was obtained (yield = 69%). ^{1}H-NMR (ppm, $CDCl_3$), δ = 6.95 (2H, H^9), 6.84 (2H, H^5), 6.79 (2H, H^{10}), 3.77 (6H, H^6), 3.12 (2H, H^2), 3.00 (4H, H^{12}), 2.81 (4H, H^3), 2.77 (2H, H^1), 2.52 (2H, H^1). ^{13}C-NMR (ppm, $CDCl_3$), δ = 170.2 (C^{11}), 150.7 (C^8), 138.2 (C^7), 136.2 (C^4), 122.5 (C^9), 120.9 (C^{10}), 113.0 (C^5), 55.7 (C^6), 52.2 (C^2), 46.7 (C^1), 38.5 (C^3), 28.9 (C^{12}). Melting point: 89.4–97.9 °C (onset–offset temperature in the DSC thermogram). HR-MS (ESI-MS) *m*/*z*: [Na+] calcd for $C_{24}H_{26}O_8Na$ 465.15; anal. 465.1515. FTIR (KBr): ν (cm^{-1}) = 1753 (C=O stretch of the carbonyl group), 915 (C–O stretch of the oxirane group), and 831 (C–O–C stretch of epoxide).

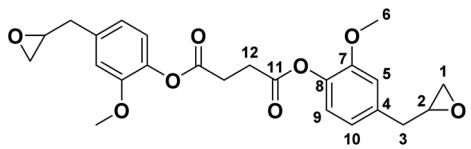

Synthesis of bis(2-methoxy-4-(oxiran-2-ylmethyl)phenyl) adipate (2)

2 was prepared by using the same procedure as that for **1** except for **1a** being replaced by **2a**, and a white solid **2** was obtained (yield = 70%). ^{1}H-NMR (ppm, $CDCl_3$), δ = 6.95 (2H, H^9), 6.84 (2H, H^5), 6.79 (2H, H^{10}), 3.80 (6H, H^6), 3.12 (2H, H^2), 2.82 (4H, H^3), 2.79 (2H, H^1), 2.63 (4H, H^{12}), 2.54 (2H, H^1), 1.89 (4H, H^{13}). ^{13}C-NMR (ppm, $CDCl_3$), δ = 171.4 (C^{11}), 150.8 (C^8), 138.4 (C^7), 136.1 (C^4), 122.6 (C^9), 121.0 (C^{10}), 113.0 (C^5), 55.7 (C^6), 52.3 (C^2), 46.8 (C^1), 38.6 (C^3), 38.6 (C^{12}), 24.3 (C^{13}). Melting point: 89.4–97.9 °C (onset–offset temperature in the DSC thermogram). HR-MS (ESI-MS) *m*/*z*: [Na+] calcd for $C_{26}H_{30}O_8Na$ 493.18; anal. 493.1825. FTIR (KBr): ν (cm^{-1}) = 1755 (C=O stretch of the carbonyl group), 935 (C–O stretch of the oxirane group), and 844 (C–O–C stretch of epoxide).

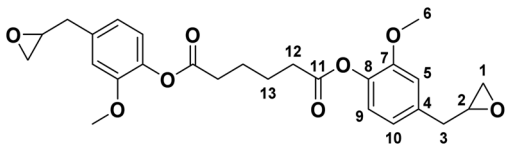

Synthesis of bis(2-methoxy-4-(oxiran-2-ylmethyl)phenyl) octanedioate (3)

3 was prepared by using the same procedure as that for **1** except for **1a** being replaced by **3a**, and a light yellow solid **3** was obtained (yield = 65%). ^{1}H-NMR (ppm, $CDCl_3$), δ = 6.93 (2H, H^9), 6.84 (2H, H^5), 6.80 (2H, H^{10}), 3.80 (6H, H^6), 3.13 (2H, H^2), 2.82 (4H, H^3), 2.78 (2H, H^1), 2.57 (4H, H^{12}), 2.53 (2H, H^1), 1.78 (4H, H^{13}), 1.48 (4H, H^{14}). ^{13}C-NMR (ppm, $CDCl_3$), δ = 171.8 (C^{11}), 150.9 (C^8), 138.4 (C^7), 136.0 (C^4), 122.6 (C^9), 121.0 (C^{10}), 113.1 (C^5), 55.8 (C^6), 52.3 (C^2), 46.8 (C^1), 38.6 (C^3), 33.9 (C^{12}), 28.6 (C^{14}), 24.8 (C^{13}). Melting point: 100.0–104.8 °C (onset–offset temperature in the DSC thermogram). HR-MS (ESI-MS) *m*/*z*: [Na+] calcd for $C_{28}H_{34}O_8Na$ 521.21; anal. 521.2139. FTIR (KBr): ν (cm^{-1}) = 1754 (C=O stretch of the carbonyl group), 922 (C–O stretch of epoxide), and 835 (C–O–C stretch of epoxide).

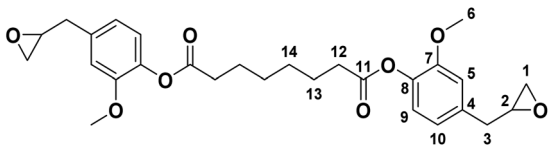

Synthesis of bis(2-methoxy-4-(oxiran-2-ylmethyl)phenyl) furan-2,5-dicarboxylate (4)

4 was prepared by using the same procedure as that for **1** except for **1a** being replaced by **4a**, and a transparent orange solid **4** was obtained (yield = 67%). ^{1}H-NMR (ppm, $CDCl_3$), δ = 7.44 (2H, H^{13}), 7.06 (2H, H^9), 6.88 (2H, H^5), 6.84 (2H, H^{10}), 3.80 (6H, H^6), 3.15 (2H, H^2), 2.84 (4H, H^3), 2.79 (2H, H^1), 2.54 (2H, H^1). ^{13}C-NMR (ppm, $CDCl_3$), δ = 155.7 (C^{11}), 150.8 (C^{12}), 146.4 (C^8), 137.5 (C^7), 136.8 (C^4), 122.4 (C^9), 121.0 (C^{10}), 119.8 (C^{13}), 113.2 (C^5), 55.8 (C^6), 52.2 (C^2), 46.7 (C^1), 38.6 (C^3). HR-MS (ESI-MS) *m*/*z*: [Na+] calcd for $C_{26}H_{24}O_9Na$ 503.13; anal. 503.1312. FTIR (KBr): ν (cm^{-1}) = 1754, 1742 (C=O stretch of the carbonyl group), 956 (C–O stretch of the oxirane group), and 839 (C–O–C stretch of epoxide).

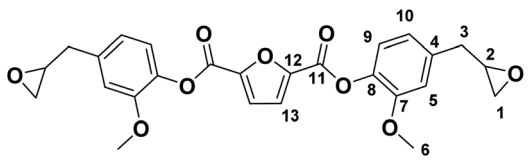

Epoxy thermoset synthesis *via* the self-curing reaction

Self-curing of **1–4** was performed by heating **1–4** with 0.5 wt% DMAP at a heating stage at 130–150 °C until a homogeneous,

viscous liquid was obtained. Then, curing was performed at 160 °C, 180 °C, and 200 °C for 2 h at each temperature under a nitrogen atmosphere. The samples were named SC(**1**)–SC(**4**), respectively. SC means self-curing. In some cases, the four thermosets are expressed as SC(**x**), **x** = **1–4**.

Epoxy thermoset synthesis *via* the diamine-curing reaction

In addition to the self-curing of **1–4**, we also investigated the curing of **1–4** with a common diamine, diaminodiphenylmethane (DDM), for the comparison of structure–properties. The curing of **1–4** with DDM was exemplified by the curing of **1** and DDM. **1** 2.00 g, and DDM 0.45 g were stirred on a heating stage at 120–130 °C until a homogeneous, viscous liquid was obtained. Then, curing was performed at 140 °C and 160 °C for 2 h at each temperature. The thermosets were named (**1**)/DDM–(**4**)/DDM, respectively. In some cases, the four thermosets are expressed as (**x**)/DDM, **x** = **1–4**.

Results and discussion

Synthesis and characterization of 1–4

Fully bio-based epoxy compounds were prepared by a two-step procedure from eugenol. The first step is the esterification of eugenol with succinyl, adipoyl, suberoyl, and 2,5-furan chloride, respectively, in ethyl acetate using triethylamine as a base, forming the intermediates **1a–4a**. The second step is the oxidation of the allylic groups of **1a–4a** by *m*-CBPA in ethyl acetate, forming epoxy compounds **1–4** (Scheme 1).

Fig. 1 displays the ^{1}H-NMR spectra of **1a–4a** in $CDCl_3$. The characteristic signals of the allylic group at 3.36 ppm (H^3), 5.08 ppm (H^1), and 5.94 ppm (H^2) were observed. The structures were further confirmed by the ^{13}C-NMR spectra (Fig. 2). The signal of the carbonyl group was observed at 171 ppm for **1–3** and at 155 ppm for **4**. The characteristic signals of the allylic group were observed at 40.1 ppm (C^3), 116.1 ppm (C^1) and 137.0 ppm (C^2), respectively, confirming the integrity of the allylic structures.

Fig. 3 displays the resulting ^{1}H-NMR spectra of **1–4** in $CDCl_3$. The signals from the allylic group disappeared while new signals due to epoxide at 2.5–3.2 ppm appeared. Fig. 4 shows the ^{13}C-NMR spectra of **1–4** in $CDCl_3$. The signals of the allylic group disappeared while the signals of epoxide appeared at 38.5 (C^3), 46.6 (C^1), and 52.2 (C^2). ^{1}H and ^{13}C-NMR spectra support the structures of **1–4**.

Fig. S1† shows the IR spectra of **1a–4a** and **1–4**. The C=C absorption of the allylic group was observed at around 1638 cm^{-1} in **1a–4a** but disappeared in **1–4**. The absorptions of epoxide were observed at around 930 and 835 cm^{-1}. The detailed information regarding the carbonyl absorption will be discussed later.

Model reaction

In our previous work, we performed a model reaction of phenyl acetate and glycidyl phenyl ether at 120 °C in the presence of DMAP. We found that the reaction was carried out through the reaction of an active ester and epoxide, as shown

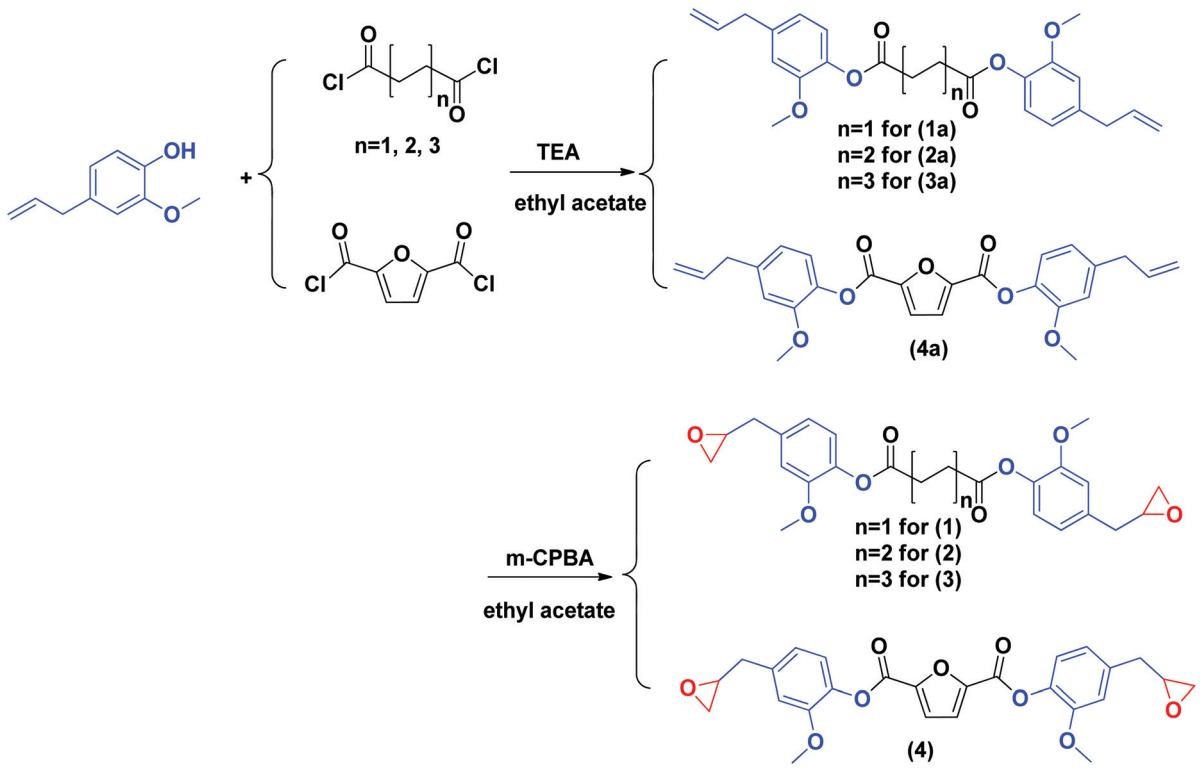

Scheme 1 Synthesis of fully bio-based epoxy compounds **1–4**.

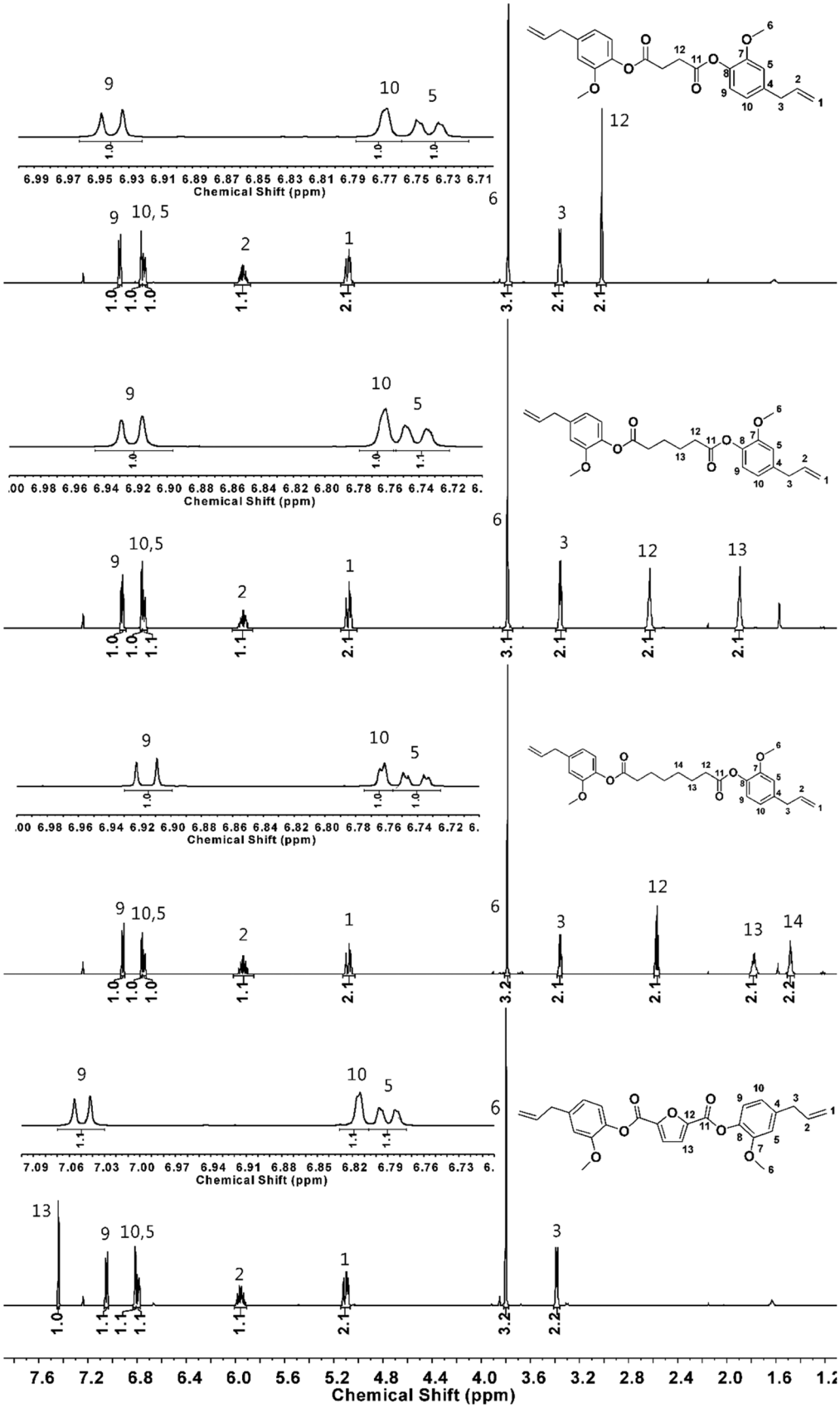

Fig. 1 ^{1}H-NMR spectra of **1a–4a**.

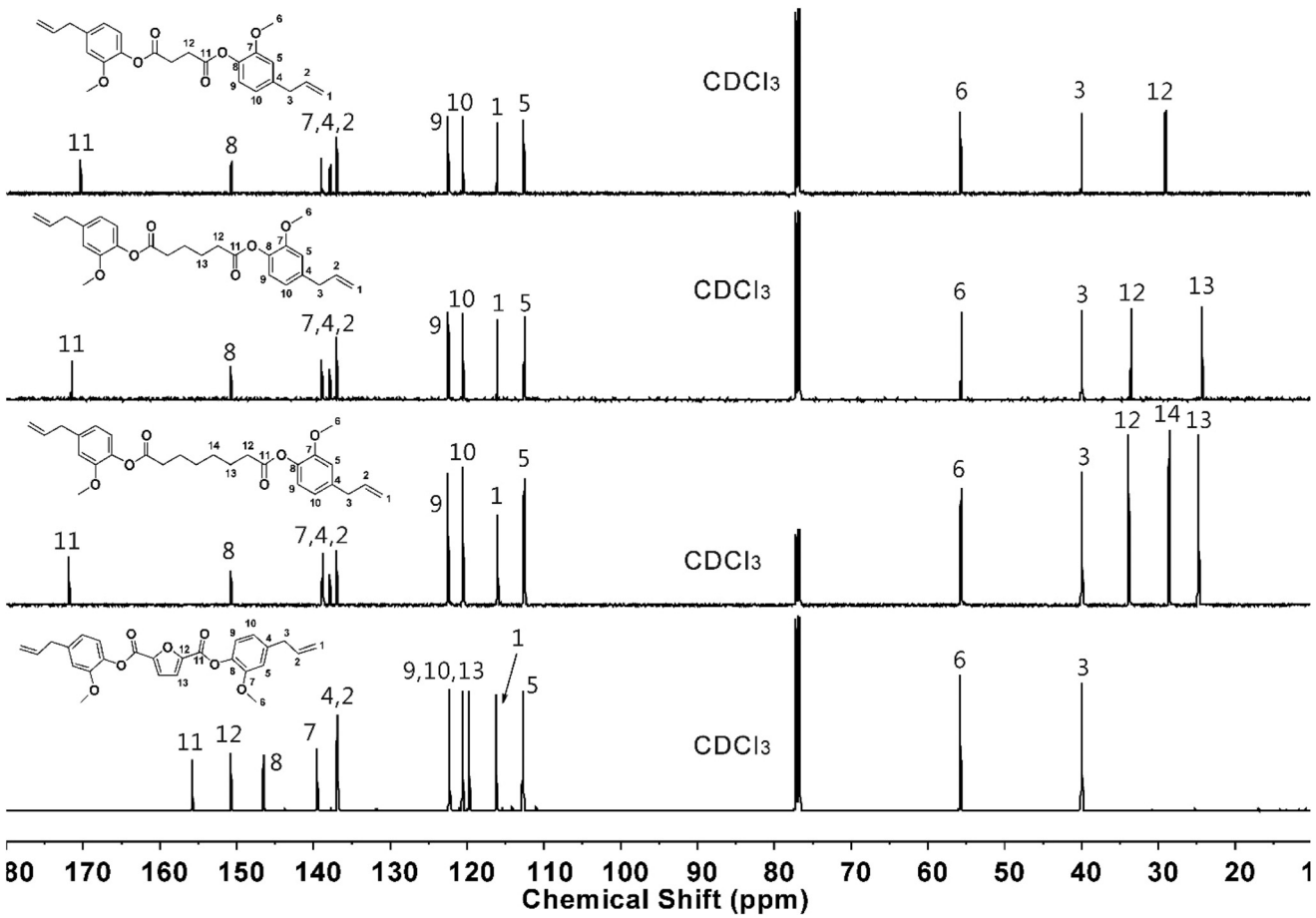

Fig. 2 ^{13}C-NMR spectra of **1a–4a** in $CDCl_3$.

in Scheme 2(a).[47] Since **1–3** are phenyl succinate, adipate, and octanedioate, respectively, they exhibited structures of phenyl-O–C(=O)–R (R = C_4, C_6, and C_8, respectively), which are structurally similar to phenyl acetate (phenyl-O–C(=O)–CH_3). Therefore, the self-curing of **1–3** should occur through the reaction of the built-in active ester and epoxide, similar to that shown in Scheme 2(a). However, **4** is a phenyl furan carboxylate, with a structure of phenyl-O–C(=O)-furan, which is structurally different from phenyl acetate. Therefore, we performed a model reaction of phenyl furan-2-carboxylate and glycidyl phenyl ether in the presence of DMAP (Scheme 2b) to evaluate the reaction route.

Fig. 5 shows the ^{1}H-NMR spectra of the model reaction at 120 °C for various periods of reaction time. The signals of the furan group from the unreactive mixture were assigned at 8.1 (H^a), 7.6 (H^c), and 6.8 (H^b) ppm, respectively, and the signals of the epoxide were assigned at 2.7–4.3 ppm (H^g, H^h, and H^i) as shown in Fig. 5 (R.T.). As the reaction progresses, the signals of the epoxide at 2.7–4.3 ppm disappeared and the signals of the furan upshifted to 8.0 ($H^{a'}$), 7.3 ($H^{c'}$), and 6.7 ($H^{b'}$), respectively. The signals of methylene and methine also appeared at 4.4 ($H^{g'}$) and 5.7 ($H^{h'}$) ppm, respectively (Fig. 5, 10–60 min). The signal of H^e at 7.5 ppm disappeared after 30 min. In order to further confirm the structure, Fig. 6 illustrates the ^{1}H–^{1}H COSY NMR spectrum of the reaction at 60 min. The correlation at 4.4/5.7 ppm (corresponds to $H^{g'}$/$H^{h'}$), at 6.7/7.3 ppm (corresponds to $H^{b'}$/$H^{c'}$), at 6.7/8.0 ppm (corresponds to $H^{b'}$/$H^{a'}$) and at 7.0/7.3 ppm (corresponds to $H^{d'}$/$H^{e'}$) confirmed our prediction in Scheme 2(b), indicating the reaction of the phenyl furan carboxylate and epoxide. Therefore, the self-curing of **4** should occur through the reaction of the built-in active ester and epoxide, similar to that shown in Scheme 2(b).

DSC thermograms

Compounds **1–4** are designed to exhibit both active esters and epoxides in the structure, so, according to the chemistry in Scheme 2, we think that they would be self-curable in the presence of DMAP. Fig. 7 displays the DSC thermograms of **1–4** without DMAP (a) and with 0.5 wt% DMAP (b). No exothermic peaks are observed in Fig. 7(a), indicating that the reactions of the active ester and epoxide did not occur without a catalyst. In Fig. 7(b), exothermic peaks at 165, 169, 182, and 177 °C, respectively, with exothermic enthalpies of around 140 kJ mol^{-1} were observed, indicating that **1–4** carried out the self-curing reaction in the presence of DMAP. For comparison, the

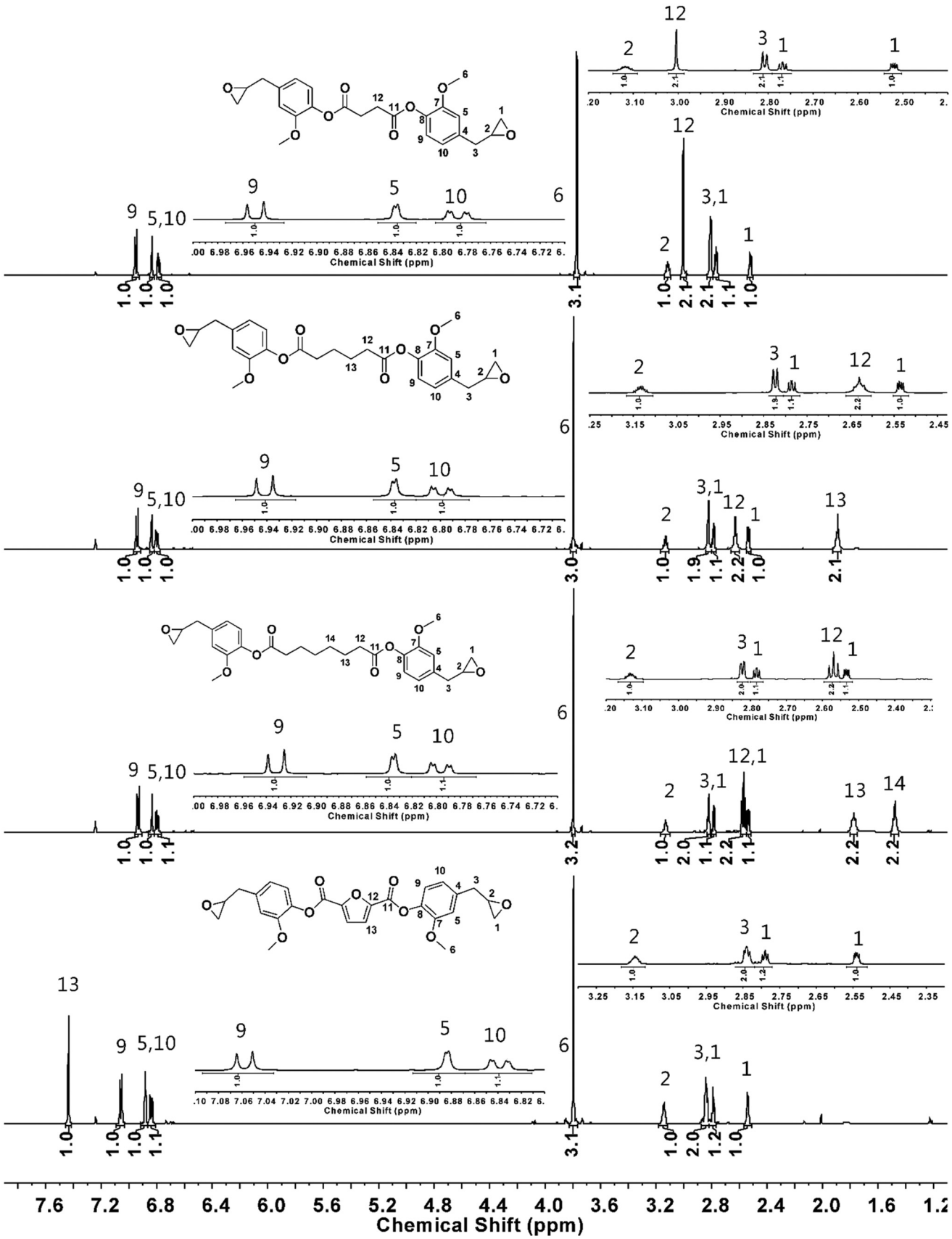

Fig. 3 ^{1}H-NMR spectra of **1–4**.

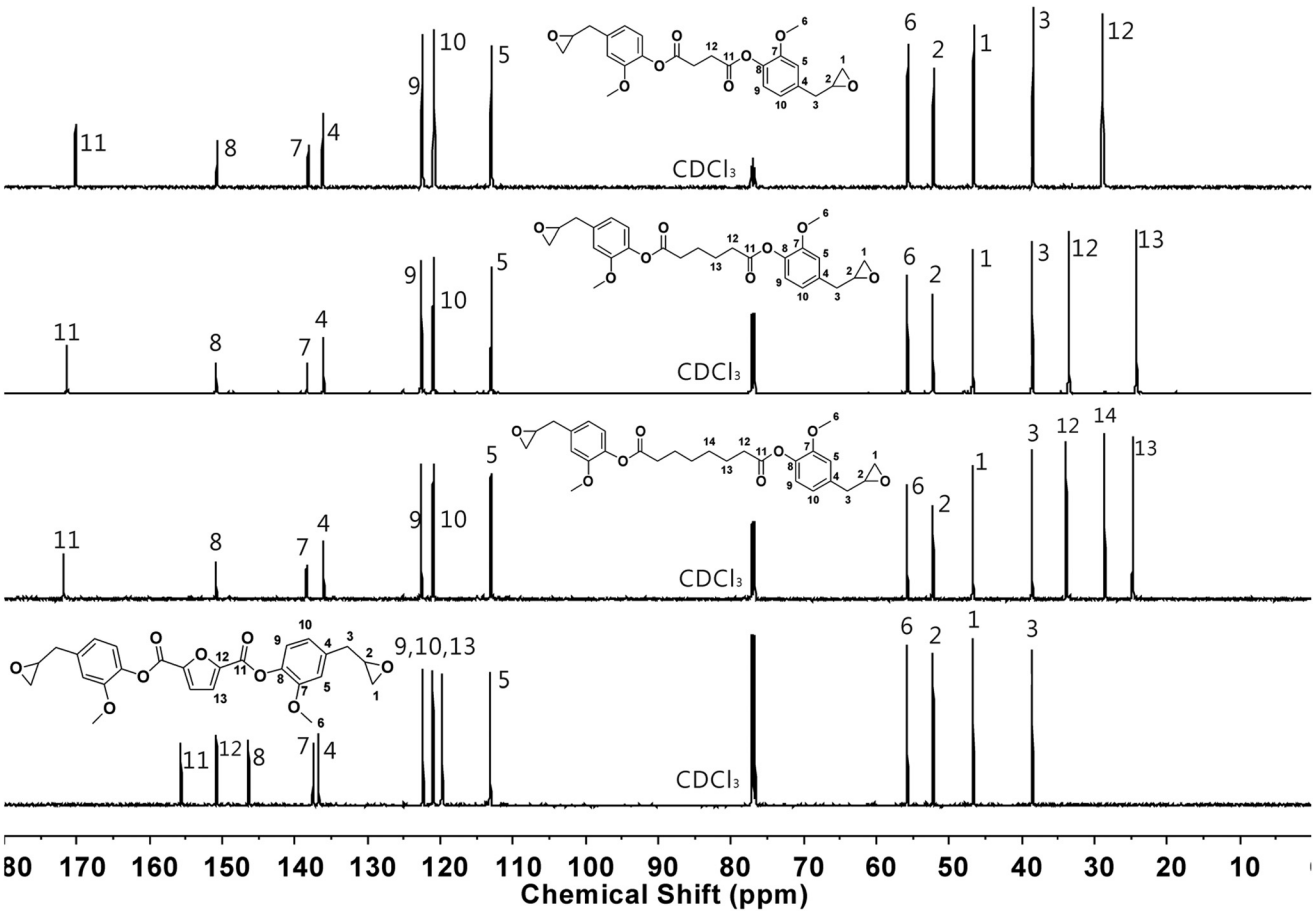

Fig. 4 ^{13}C-NMR spectra of **1–4** in $CDCl_3$.

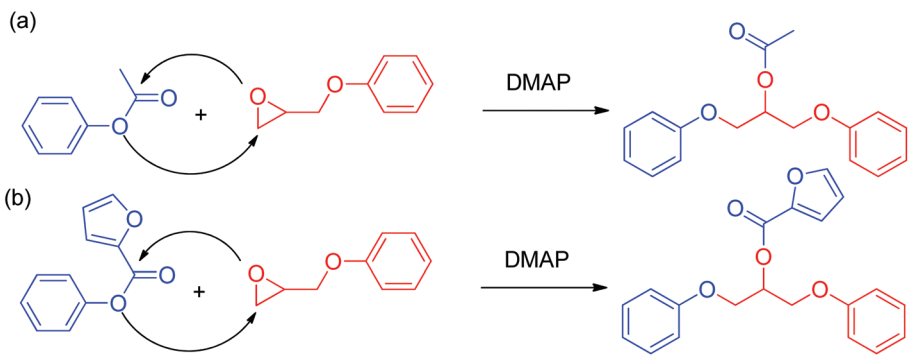

Scheme 2 The reaction of glycidyl phenyl ether with (a) phenyl acetate and (b) phenyl furan-2-carboxylate in the presence of DMAP.

DSC thermogram of DGEBA with 0.5 wt% DMAP is also given in Fig. 7(b). An exotherm with a peak temperature of 113 °C and an exothermic enthalpy of 140 kJ mol^{-1} was observed. The exotherm is thought to be related to the homopolymerization of epoxide groups.[48] However, if we compare the thermograms of **1–4** and DGEBA in Fig. 7(b), we can find that no exotherm around 113 °C for **1**, **3** and **4**(note that **2** is difficult to interpret due to its melting point at 110 °C) was observed. That is, the homopolymerization of epoxide in **1–4** did not occur, showing a high selectivity between active esters and epoxides. This high selectivity is consistent with the good purity of the reaction product shown in Fig. 6.

FTIR spectra and the proposed curing mechanism

As shown in the model reaction (Scheme 2), the reaction between active esters and epoxide led to a change of the ester group from an aromatic ester (phenyl-O–C(=O)–) to an aliphatic ester (isopropyl-O–C(=O)–). In IR spectroscopy, an ali-

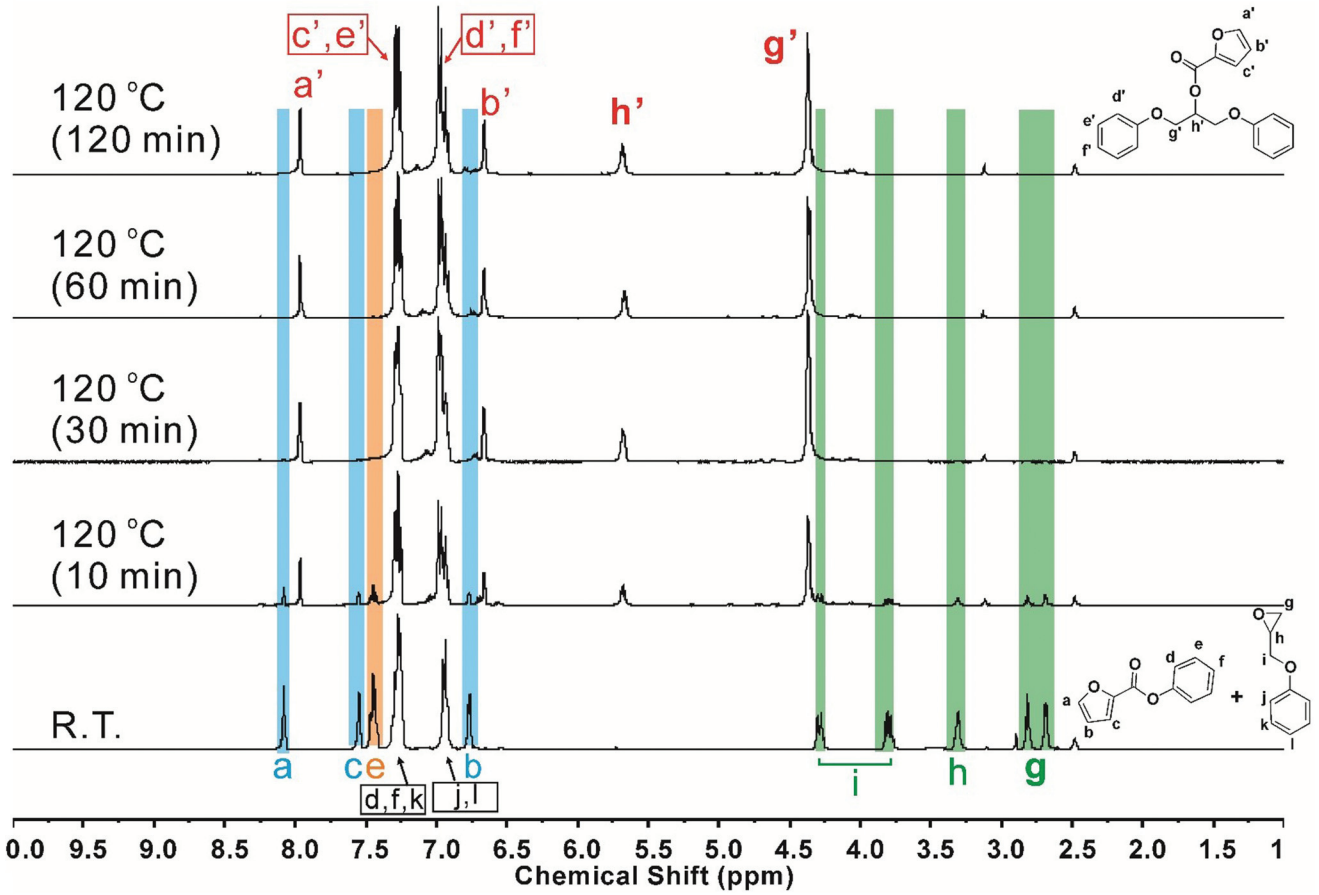

Fig. 5 Time-dependent ^{1}H-NMR spectra of the model reaction.

phatic ester has a lower absorption wavenumber than an aromatic ester does. Fig. 8 shows the IR spectra of **1–4** before and after curing. The carbonyl absorption upshifted from 1757 cm^{-1} to 1727 cm^{-1} for **1–3** after curing. The carbonyl absorption upshifted from 1759 and 1742 cm^{-1} (asymmetric and symmetric stretch) to 1740 and 1718 cm^{-1} for **4**. This result indicates that the ester group has changed from an aromatic ester to an aliphatic ester, further supporting the self-curing reaction of **1–4**. The self-curing reaction of (**x**) to SC(**x**) is expressed in Scheme 3(a), in which the reaction between epoxides and active esters led to an epoxy network. In this mechanism, DMAP attacked the epoxide and formed an alkoxy anion in step 1. The alkoxy anion attacked the ester group and released a phenoxy anion in step 2. The phenoxy anion attacked the carbon of the C–N bond in step 3, releasing DMAP that will catalyze another epoxide moiety. The alkoxy anion formed in step 1 further attacked the other ester group and gradually led to a network (steps 4 and 5, and further reactions). For property comparison, we also cured **1–4** by DDM, forming the (**x**)/DDM thermosets in Scheme 3(b). The reaction between epoxides and amines forms hydroxyl groups and led to the formation of an epoxy network. The IR spectra of (**x**)/DDM are shown in Fig. 8. An obvious signal of a hydroxyl group was observed at 3385 cm^{-1} for (**x**)/DDM. The signal of a carbonyl group is present at the same position as that of (**x**), indicating that active esters do not participate in the cross-linking reaction. Table 1 lists the gel content of SC(**x**). The gel content is larger than 98% for each sample. Also, the chloroform solution remained transparent after the test. The two observations indicated that a network was formed in each SC (**x**), supporting the self-curing reaction of **1–4** to epoxy networks.

Thermal properties

Fig. 9(a) shows the DSC thermograms of the self-curing epoxy thermosets, SC(**x**). The T_g values are 114, 88, 73, and 147 °C, respectively. No exothermic peaks are observed in the figure, indicating that they were fully cured. The DMA thermograms of SC(**x**) are displayed in Fig. 9(b). There are modulus plateaus for SC(**1**)–SC(**4**) after glass relaxation, indicating that they belong to thermosets. The T_g values, defined by the peak temperature of the tan δ curve, are 131, 107, 92 and 161 °C, respectively. For SC(**1**)–SC(**3**), the T_g values decreased with the increasing chain length of the diacid. The SC(**4**), due do the higher rigidity of furan than alkylene, exhibited the highest T_g. Fig. 10 displays the TGA thermograms of SC(**x**). Depending on the structure, the T_{d5} (5 wt% degradation temperatures) are in the range of 350–392 °C (Table 1). The char yields (CY) at

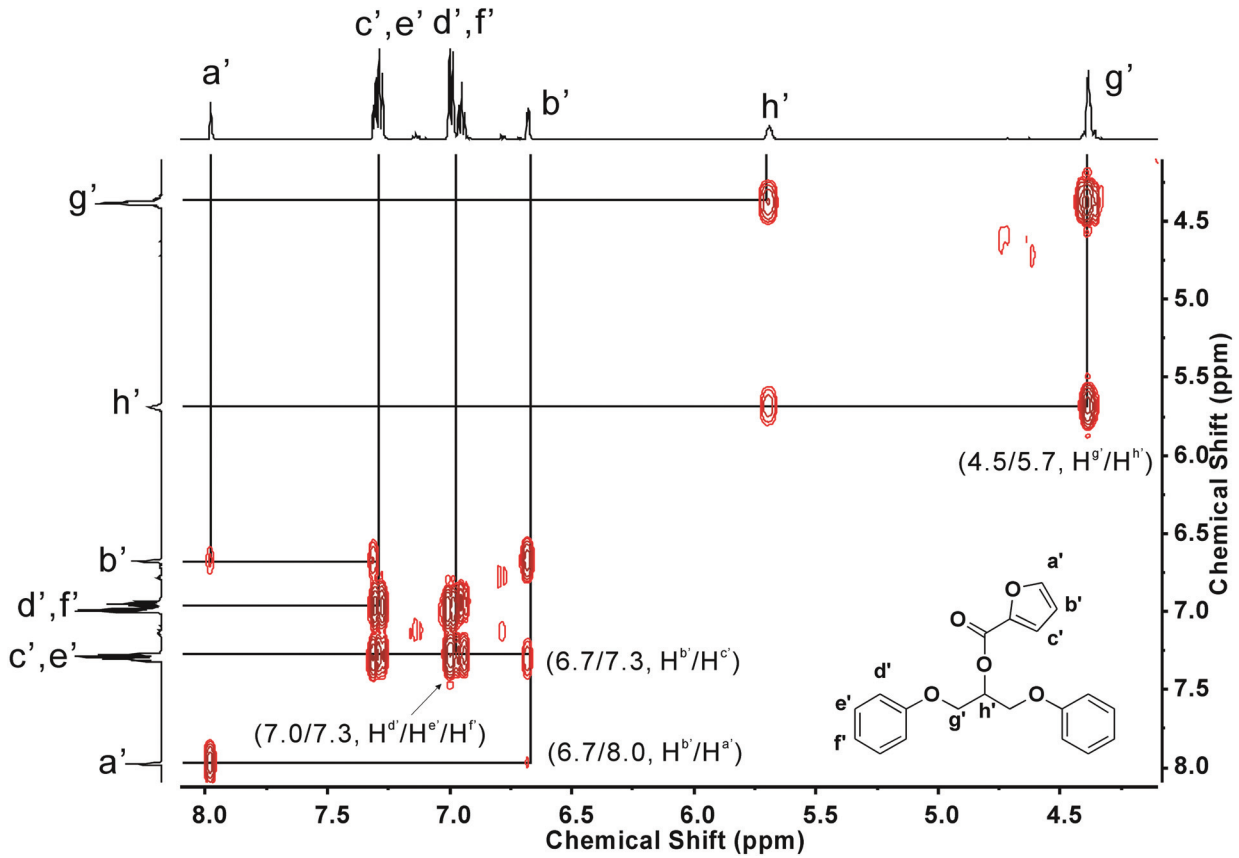

Fig. 6 $^{1}H-^{1}H$ COSY NMR spectrum of the reaction product of the model reaction at 60 min in DMSO-d_6.

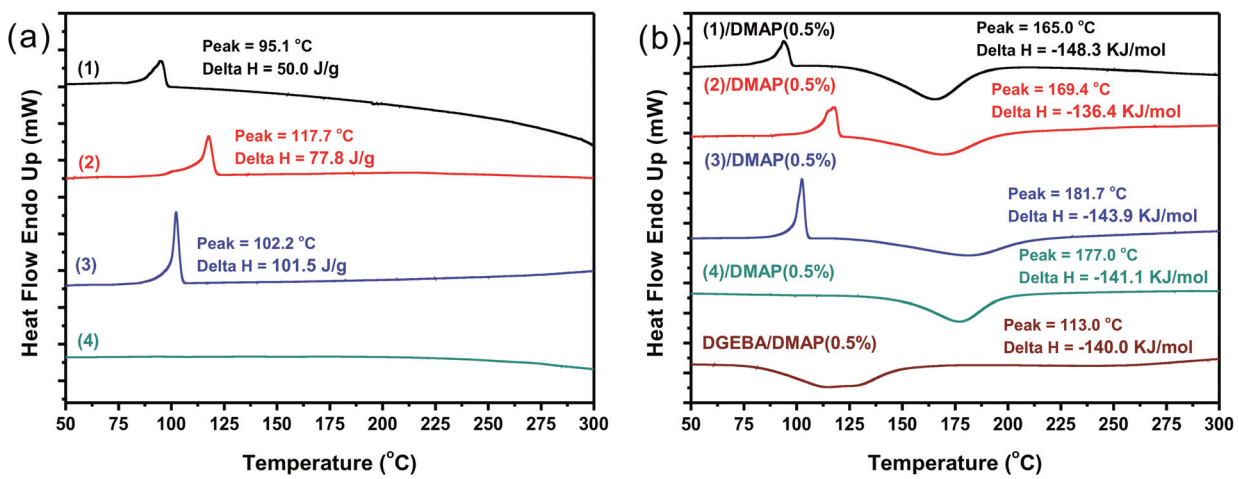

Fig. 7 DSC thermograms of **1–4** without DMAP (a) and with 0.5 wt% DMAP (b). DGEBA with 0.5 wt% DMAP was also included 4(b).

800 °C are in the range of 17–27%. As for the mechanical properties, we have tried to measure the mechanical properties of the thermosets. Fig. S2† shows a typical stress–strain curve of SC(**3**) and (**3**)/DDM. Unfortunately, we observed that the test stopped after the force reached the maximum loading force of the instrument (100 Nt). Therefore, no exact data on tensile strength and elongation at break were reported here. However, we have observed that the initial modulus of SC(**3**) is 1.86 GPa, which is much larger than that (0.78 GPa) of (**3**)/DDM. The result demonstrates the advantage of the self-curing thermoset in rigidity.

The DSC, DMA, and TGA thermograms of (**x**)/DDM are shown in Fig. S3 and S4† for property comparison. The thermal properties of all thermosets are listed in Table 1. (**x**)/

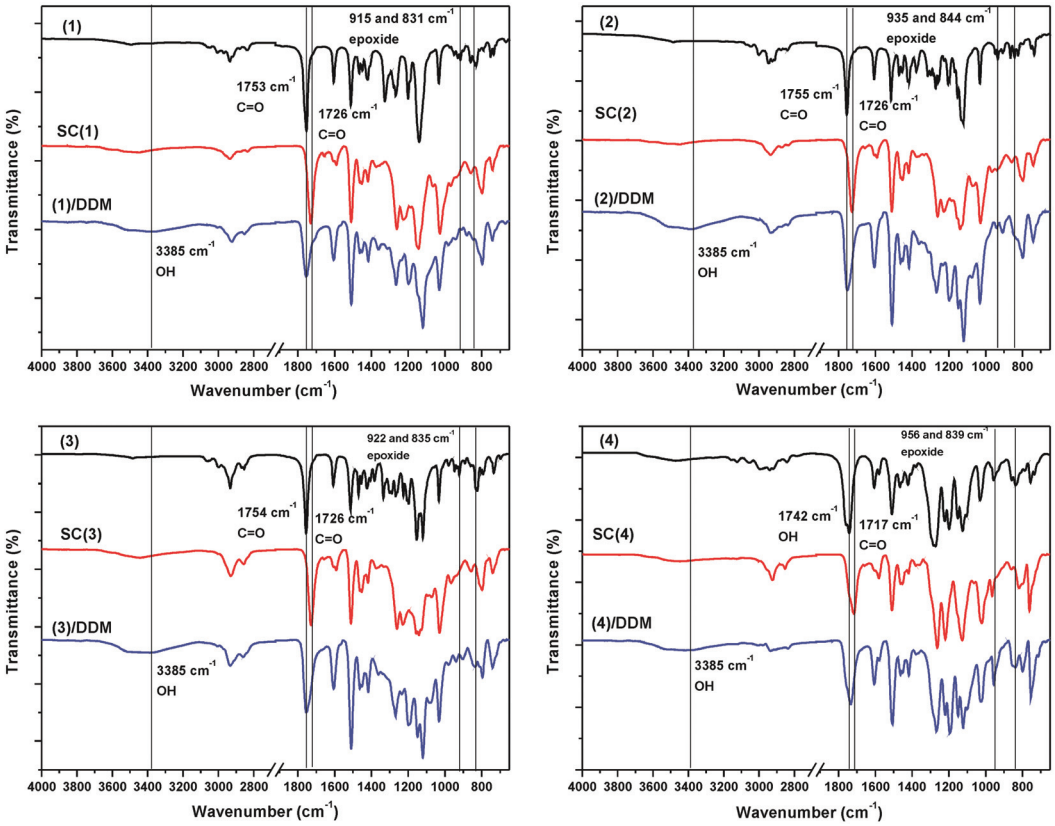

Fig. 8 FTIR spectra of (x), SC(x) and (x)/DDM. x = 1–4.

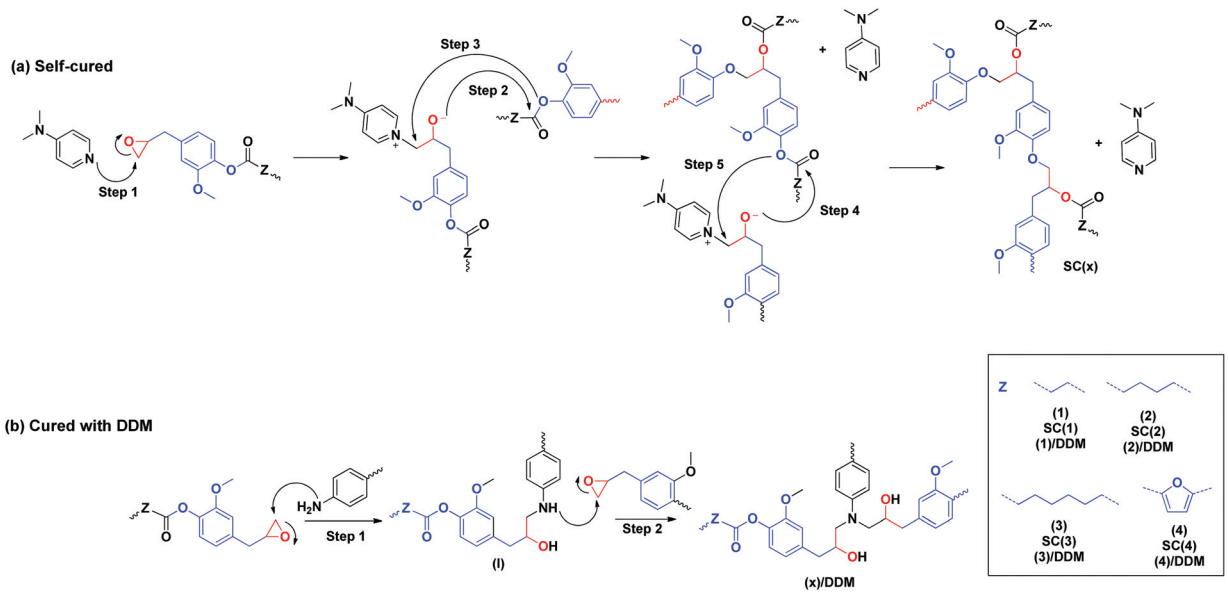

Scheme 3 Parts of the structures of (a) SC(x) and (b) (x)/DDM. x = 1–4.

DDM shows T_g 8–20 °C higher than that of SC(x), probably due to the rigid diphenylmethane structure. However, (x)/DDM shows a much lower rubbery modulus than SC(x) for x = 1–3, demonstrating the higher rigidity of SC(x) after the glass transition. For example, the rubbery modulus is 15 MPa for (2)/DDM and 52 MPa for SC(2). The lower rigidity of (x)/DDM at the rubbery state can also be supported by the higher height of the tan δ curve, as listed in Table 1. This indicates that the

Table 1 Thermal and dielectric properties of SC(x) and (x)/DDM

Sample	GC[a] (%)	T_g (°C) (DSC)[b]	T_g (°C) (DMA)[c]	Rubbery E' [d] (MPa)	Height of tan δ	$T_{d5\%}$ [e] (°C)	CY[f] (%)	D_k[g]	D_f[h]
SC(**1**)	>98	114	131	42	0.60	370	17	3.10	0.007
(**1**)/DDM	>98	118	139	18	0.98	364	24	3.03	0.019
SC(**2**)	>98	88	107	52	0.66	395	27	3.08	0.008
(**2**)/DDM	>98	99	120	15	1.03	350	20	3.05	0.022
SC(**3**)	>98	73	92	29	0.70	392	17	3.01	0.008
(**3**)/DDM	>98	91	112	21	1.03	368	25	3.08	0.017
SC(**4**)	>99	147	161	32	0.61	350	24	3.15	0.010
(**4**)/DDM	>99	169	181	36	0.74	341	28	3.10	0.020

[a] The gel content tested in chloroform. [b] The T_g was determined at the half height of the step in a DSC thermogram. [c] The peak temperature of a tan δ curve in a DMA thermogram. [d] The storage modulus at the rubbery state was determined at T_g +30 °C. [e] 5% decomposition temperature in a TGA thermogram. [f] The char yield at 800 °C in a TGA thermogram (wt%). [g] The dielectric constant measured at 1 GHz at room temperature. [h] The dissipation factor measured at 1 GHz at room temperature.

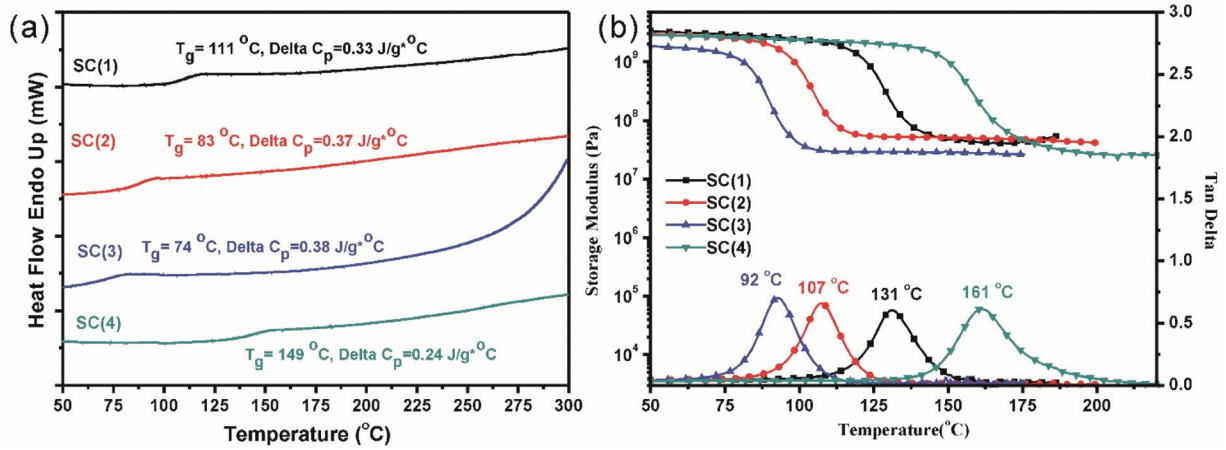

Fig. 9 (a) DSC and (b) DMA thermograms of SC(x). x = **1**–**4**.

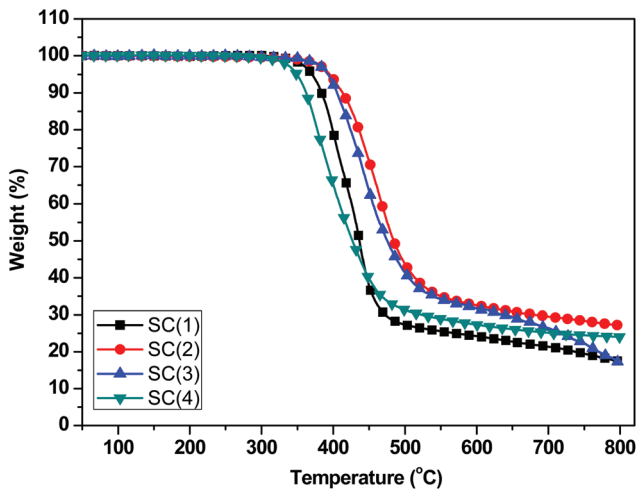

Fig. 10 TGA thermograms of SC(x). x = **1**–**4**.

packing of SC(x) is more compact than that of (x)/DDM for x = **1**–**3**. The interaction between the secondary alcohol and furan might explain the slightly higher rubbery modulus of (**4**)/DDM than that of SC(**4**). The hydrogen bonding between furan and secondary alcohol groups reinforces the thermomechanical properties of (**4**)/DDM. The signal at 1102 cm^{-1} (C–O–C of furan) up-shifted to 1098 cm^{-1} in (**4**)/DDM (Fig. S5†). The up-shifts in the wavenumber indicate an interaction between the furan and secondary alcohol groups, which is supported by Palmese *et al.*[49] TGA data show that (x)/DDM displays a lower 5 wt% decomposition temperature than SC(x). For example, 5 wt% decomposition temperature is 350 °C for (**2**)/DDM and is 395 °C for SC(**2**), demonstrating the advantage of the self-curing strategy on the thermal stability.

Dielectric properties

Table 1 also lists the dielectric properties of all thermosets. The dielectric constants of SC(x) 3.0–3.1, which are approximately the same as those of (x)/DDM. dissipation factors of SC (x) are only 0.007–0.010, which are 50–63% lower than those of (x)/DDM. The highly-polar secondary alcohol, as evidenced by the hydroxyl absorption at 3385 cm^{-1} in Fig. 8, is responsible for the high dissipation factors of (x)/DDM. In contrast, no secondary alcohol was formed for SC(x), according to the curing chemistry and the lack of hydroxyl absorption at 3385 cm^{-1} in Fig. 8. In a circuit, the signal propagation loss is proportional to the frequency, dissipation factor, and the square root of the

dielectric constant.[50,51] Therefore, a dielectric material with a low dielectric constant and dissipation factor, especially with a low dissipation factor, is desired. This result demonstrates the advantage of self-cured epoxy thermosets in signal propagation loss in a circuit.

Conclusions

We have successfully prepared four fully bio-based epoxy compounds **1–4** from eugenol through the esterification of the phenolic group, followed by the oxidation of the allylic group. Through this method, the active ester and epoxide moieties were simultaneously integrated into each compound. According to the NMR analysis (Fig. 5) of a model reaction of glycidyl phenyl ether and phenyl furan-2-carboxylate, we confirmed that the active ester and epoxide could react with each other. According to the obvious exotherms in the DSC thermograms (Fig. 7) and the shift of carbonyl absorption in the IR spectra (Fig. 8), we reported the DMAP-catalyzed self-curing reaction of **1–4**. Fully bio-based epoxy thermosets were achieved according to this chemistry. The self-cured epoxy thermosets, SC(**x**), show better properties than the DDM-cured thermosets, (**x**)/DDM, except for a slight reduction in the T_g values. Especially, due to the lack of secondary alcohols, the dissipation factors of SC(**x**) were 50–63% lower than (**x**)/DDM, demonstrating the advantage of SC(**x**) in signal propagation loss in a circuit. In short, a strategy for preparing fully bio-based epoxy thermosets with low dissipation factors is revealed in this work.

Conflicts of interest

The authors declare no competing financial interest.

Acknowledgements

This work was financially supported by the "Advanced Research Center For Green Materials Science and Technology" from The Featured Area Research Center Program within the framework of the Higher Education Sprout Project by the Ministry of Education (107L9006) and the Ministry of Science and Technology in Taiwan (MOST 107-3017-F-002-001 and 107-2221-E-005-025-MY3).

Notes and references

1 R. P. Babu, K. O'Connor and R. Seeram, *Prog. Biomater.*, 2013, **2**, 8.
2 A. Gandini and T. M. Lacerda, *Prog. Polym. Sci.*, 2015, **48**, 1–39.
3 S. Sen, S. Patil and D. S. Argyropoulos, *Green Chem.*, 2015, **17**, 4862–4887.
4 G. Z. Papageorgiou, D. G. Papageorgiou, Z. Terzopoulou and D. N. Bikiaris, *Eur. Polym. J.*, 2016, **83**, 202–229.
5 R. Beerthuis, G. Rothenberg and N. R. Shiju, *Green Chem.*, 2015, **17**, 1341–1361.
6 S. Muñoz-Guerra, C. Lavilla, C. Japu and A. Martínez de Ilarduya, *Green Chem.*, 2014, **16**, 1716–1739.
7 F. H. Isikgor and C. R. Becer, *Polym. Chem.*, 2015, **6**, 4497–4559.
8 S. Hu, Z. Zhang, Y. Zhou, J. Song, H. Fan and B. Han, *Green Chem.*, 2009, **11**, 873–877.
9 H. Fan, Y. Yang, J. Song, G. Ding, C. Wu, G. Yang and B. Han, *Green Chem.*, 2014, **16**, 600–604.
10 S. Hu, Z. Zhang, J. Song, Y. Zhou and B. Han, *Green Chem.*, 2009, **11**, 1746–1749.
11 L. Wu, J. Song, B. Zhang, B. Zhou, H. Zhou, H. Fan, Y. Yang and B. Han, *Green Chem.*, 2014, **16**, 3935–3941.
12 H. Lee and K. Neville, *Handbook of epoxy resins*, 1967.
13 Y. L. Liu, C. S. Wu, K. Y. Hsu and T. C. Chang, *J. Polym. Sci., Part A: Polym. Chem.*, 2002, **40**, 2329–2339.
14 S. Wang, S. Ma, Q. Li, X. Xu, B. Wang, W. Yuan, S. Zhou, S. You and J. Zhu, *Green Chem.*, 2019, **21**, 1484–1497.
15 M. Decostanzi, R. Auvergne, B. Boutevin and S. Caillol, *Green Chem.*, 2019, **21**, 724–747.
16 E. D. Hernandez, A. W. Bassett, J. M. Sadler, J. J. La Scala and J. F. Stanzione, *ACS Sustainable Chem. Eng.*, 2016, **4**, 4328–4339.
17 D. Fourcade, B. S. Ritter, P. Walter, R. Schönfeld and R. Mülhaupt, *Green Chem.*, 2013, **15**, 910–918.
18 A.-S. Mora, R. Tayouo, B. Boutevin, G. David and S. Caillol, *Green Chem.*, 2018, **20**, 4075–4084.
19 J. R. Mauck, S. K. Yadav, J. M. Sadler, J. J. La Scala, G. R. Palmese, K. M. Schmalbach and J. F. Stanzione III, *Macromol. Chem. Phys.*, 2017, **218**, 1700013.
20 E. A. Baroncini, S. Kumar Yadav, G. R. Palmese and J. F. Stanzione III, *J. Appl. Polym. Sci.*, 2016, **133**, 44103.
21 H. Nouailhas, C. Aouf, C. Le Guerneve, S. Caillol, B. Boutevin and H. Fulcrand, *J. Polym. Sci., Part A: Polym. Chem.*, 2011, **49**, 2261–2270.
22 F. Dasgupta, *WO Patent*, WO2011041487, 2011.
23 P. Livant, T. R. Webb and W. Xu, *J. Org. Chem.*, 1997, **62**, 737–742.
24 N. H. Nieu, T. T. M. Tan and N. L. Huong, *J. Appl. Polym. Sci.*, 1996, **61**, 2259–2264.
25 İ. Kaya, F. Doğan and M. Gül, *J. Appl. Polym. Sci.*, 2011, **121**, 3211–3222.
26 C. Aouf, J. Lecomte, P. Villeneuve, E. Dubreucq and H. Fulcrand, *Green Chem.*, 2012, **14**, 2328–2336.
27 R. Auvergne, S. Caillol, G. David, B. Boutevin and J.-P. Pascault, *Chem. Rev.*, 2014, **114**, 1082–1115.
28 T. Koike, *Polym. Eng. Sci.*, 2012, **52**, 701–717.
29 S. Ma, T. Li, X. Liu and J. Zhu, *Polym. Int.*, 2016, **65**, 164–173.
30 S. Ma and D. C. Webster, *Macromolecules*, 2015, **48**, 7127–7137.
31 S. Ma, C. S. Kovash and D. C. Webster, *J. Coat. Technol. Res.*, 2017, **14**, 367–375.

32 S. Ma, D. C. Webster and F. Jabeen, *Macromolecules*, 2016, **49**, 3780–3788.
33 B. Sung, S. Prasad, S. C. Gupta, S. Patchva and B. B. Aggarwal, in *Advances in Botanical Research*, ed. L.-F. Shyur and A. S. Y. Lau, Academic Press, 2012, vol. 62, pp. 57–132.
34 A. K. Tripathi and S. Mishra, in *Ecofriendly Pest Management for Food Security*, ed. Omkar, Academic Press, San Diego, 2016, pp. 507–524, DOI: 10.1016/B978-0-12-803265-7.00016-6.
35 J. Qin, H. Liu, P. Zhang, M. Wolcott and J. Zhang, *Polym. Int.*, 2014, **63**, 760–765.
36 J. Wan, B. Gan, C. Li, J. Molina-Aldareguia, Z. Li, X. Wang and D.-Y. Wang, *J. Mater. Chem. A*, 2015, **3**, 21907–21921.
37 J. Wan, B. Gan, C. Li, J. Molina-Aldareguia, E. N. Kalali, X. Wang and D.-Y. Wang, *Chem. Eng. J.*, 2016, **284**, 1080–1093.
38 J. Wan, J. Zhao, B. Gan, C. Li, J. Molina-Aldareguia, Y. Zhao, Y.-T. Pan and D.-Y. Wang, *ACS Sustainable Chem. Eng.*, 2016, **4**, 2869–2880.
39 J.-T. Miao, L. Yuan, Q. Guan, G. Liang and A. Gu, *ACS Sustainable Chem. Eng.*, 2017, **5**, 7003–7011.
40 I. Faye, M. Decostanzi, Y. Ecochard and S. Caillol, *Green Chem.*, 2017, **19**, 5236–5242.
41 F. O. Ayorinde, G. Osman, R. L. Shepard and F. T. Powers, *J. Am. Oil Chem. Soc.*, 1988, **65**, 1774–1777.
42 I. Bechthold, K. Bretz, S. Kabasci, R. Kopitzky and A. Springer, *Chem. Eng. Technol.*, 2008, **31**, 647–654.
43 D. R. Vardon, N. A. Rorrer, D. Salvachúa, A. E. Settle, C. W. Johnson, M. J. Menart, N. S. Cleveland, P. N. Ciesielski, K. X. Steirer, J. R. Dorgan and G. T. Beckham, *Green Chem.*, 2016, **18**, 3397–3413.
44 A. F. Sousa, C. Vilela, A. C. Fonseca, M. Matos, C. S. R. Freire, G.-J. M. Gruter, J. F. J. Coelho and A. J. D. Silvestre, *Polym. Chem.*, 2015, **6**, 5961–5983.
45 M. Gomes, A. Gandini, A. J. D. Silvestre and B. Reis, *J. Polym. Sci., Part A: Polym. Chem.*, 2011, **49**, 3759–3768.
46 C. K. Lee, J. S. Yu and H.-J. Lee, *J. Heterocycl. Chem.*, 2002, **39**, 1207–1217.
47 C. H. Chen, Z. C. Gu, Y. L. Tsai, R. J. Jeng and C. H. Lin, *Polymer*, 2018, **140**, 225–232.
48 I. E. Dell'Erba and R. J. J. Williams, *Polym. Eng. Sci.*, 2006, **46**, 351–359.
49 F. Hu, J. J. La Scala, J. M. Sadler and G. R. Palmese, *Macromolecules*, 2014, **47**, 3332–3342.
50 W. Volksen, R. D. Miller and G. Dubois, *Chem. Rev.*, 2010, **110**, 56–110.
51 G. Maier, *Prog. Polym. Sci.*, 2001, **26**, 3–65.